MSCA Doctorate Network

CONTRABASS

zero-CO_2 cemeNt ThRough cArBonation of cAlcium Silicates and aluminateS

Deliverable D 3.2

Gibbs-energy dataset to calculate $CaCO_3$-H_2O phase diagram + guest elements.

Funded by the European Union

"Funded by the European Union. Views and opinions expressed are, however, those of the author(s) only and do not necessarily reflect those of the European Union or the European Research Executive Agency (REA). Neither the European Union nor the granting authority can be held responsible for them."

Grant Agreement Nº:	101119715
Project name:	Zero-CO_2 cemeNt ThRough cArBonation of cAlcium Silicates and aluminateS
Project acronym:	CONTRABASS
Topic:	HORIZON-MSCA-2022-DN-01-01
Call (part) identifier:	HORIZON-MSCA-2022-DN-01
Starting date:	01/01/2024
Type of action:	HORIZON TMA MSCA Doctoral Networks
Granting authority:	European Research Executive Agency
Start date of the project:	01 January 2024
Project duration:	48 months
Project coordinator:	Hegoi Manzano (UPV/EHU)

Deliverable Nº:	3.2		
Deliverable name:	Gibbs-energy dataset to calculate $CaCO_3$-H_2O phase diagram +guest elements		
WP Nº:	3	**WP Leader:**	Alexander Pisch
Author:	Batoul Assi		
Contributors:	Alexander Pisch		
Due date:	Month 24	**Actual submission date:**	09/12/2025
Dissemination level:	PU/SEN		

This project has received funding from the European Union's Horizon Europe research and innovation programme under Grant Agreement No 101119715.

Document history		
Revision	Date	Description
1	28/11/2025	First draft
2	02/12/2025	Second Draft
3	04/12/2025	Final Draft

Report contributors		
Name	Beneficiary Short Name	Details of contribution
Batoul Assi	CNRS2	Author
Alexander Pisch	CNRS2	Reviewer

Funded by the European Union

"Funded by the European Union. Views and opinions expressed are, however, those of the author(s) only and do not necessarily reflect those of the European Union or the European Research Executive Agency (REA). Neither the European Union nor the granting authority can be held responsible for them."

Table of Contents

Funded by the European Union

"Funded by the European Union. Views and opinions expressed are, however, those of the author(s) only and do not necessarily reflect those of the European Union or the European Research Executive Agency (REA). Neither the European Union nor the granting authority can be held responsible for them."

1. Executive Summary

This deliverable presents the development of the first version of a coherent thermodynamic Gibbs-energy dataset for $CaCO_3$ polymorphs and substituted carbonate phases, prepared for direct integration into the GEMS and FactSage thermodynamic modeling softwares. It was developed within the CONTRABASS MSCA Doctoral Network (DC5 project) to support the construction of $CaCO_3$–H_2O phase diagrams, to be the fundamental thermodynamic data for any kinetic modeling and to assess the influence of guest elements typical of cement-based systems.

The overarching aim of this work is to establish a coherent high-quality thermodynamic dataset based on state-of-the-art DFT calculations and a critical review of available experimental literature information for calcium carbonates, with and without the insertion of minor elements such as Mg, which strongly influence carbonation behavior in low-carbon cementitious materials. This first dataset includes structural, energetic, vibrational, and temperature-dependent thermodynamic properties for the three $CaCO_3$ polymorphs (calcite, aragonite, and vaterite) as well as 0K energies of their Mg-substituted counterparts.

The computational workflow combines Density Functional Theory (using the SCAN meta-GGA exchange functional) and lattice dynamics (phonon) calculations producing consistent and experimentally validated datasets of:

- optimized lattice parameters and volumes,
- 0K ground-state and formation energies,
- mixing energies along the Ca–Mg binary substitution,
- temperature-dependent thermodynamic functions Cp(T), S(T), H(T), and G(T) for the pure polymorphs.

These results form the foundation for future construction of the $CaCO_3$–H_2O phase diagrams, kinetic growth and dissolution simulations and for equilibrium modeling of substituted carbonates and carbonation products in cementitious systems using GEMS.

Major scientific insights include:

- Structural relaxations performed using the SCAN exchange–correlation functional (0K) agree remarkably well with experimental room-temperature lattice constants, with differences below 0.5%. This level of accuracy surpasses that of PBE, LDA, and hybrid functionals.
- SCAN reproduces thermodynamic properties (formation energy, heat capacity, standard entropy) with deviations less than 1% which is often within the experimental uncertainties.
- Mg substitution produces negative mixing energies at specific substitution levels in both calcite and vaterite, but not in aragonite, consistent with the structural preferences observed in natural carbonate systems
- Phonon-derived Gibbs-energies confirm the expected thermodynamic stability order and the calculated transition energies at room temperature agree with literature values for the aragonite-to-calcite and vaterite-to-calcite transformations.

The current dataset offers as well a reliable starting point for binary Ca–Mg carbonate phase diagrams at 0K and for modeling carbonation pathways relevant to low-carbon cement. Limitations remain, including uncertainties mainly in vaterite structures.

Funded by the European Union

"Funded by the European Union. Views and opinions expressed are, however, those of the author(s) only and do not necessarily reflect those of the European Union or the European Research Executive Agency (REA). Neither the European Union nor the granting authority can be held responsible for them."

Overall, this deliverable provides the methodology, validation, preliminary dataset, and roadmap for expanding to full Ca–Mg–Fe–Na multi-component carbonate systems and integrating them into GEMS and CALPHAD, forming the thermodynamic backbone of the CONTRABASS modeling platform for sustainable and CO_2-negative construction materials.

2. Abbreviations and acronyms

Abbreviation / Acronym	Description
CC	Calcium Carbonates
ACC	Amorphous Calcium Carbonates
DFT	Density Functional Theory
SCAN	Strongly Constrained and Appropriately Normed meta-GGA functional
PBE	Perdew–Burke–Ernzerhof GGA functional
VASP	Vienna Ab Initio Simulation Package

Funded by the European Union

"Funded by the European Union. Views and opinions expressed are, however, those of the author(s) only and do not necessarily reflect those of the European Union or the European Research Executive Agency (REA). Neither the European Union nor the granting authority can be held responsible for them."

3. Background

The present document constitutes the Deliverable D3.2 “Gibbs-energy dataset to calculate $CaCO_3$-H_2O phase diagram + guest elements” in the framework of the Marie Sklodowska-Curie Actions Doctoral Network Project 101119715 – CONTRABASS as described in the HORIZON-MSCA-2022-DN-01.

The construction industry is responsible for approximately 8% of global CO_2 emissions, with cement production alone contributing nearly 2.8 billion tons of CO_2 annually through calcination processes and fossil fuel combustion (Miller et al., 2016). This environmental burden, coupled with projected increases in global construction demand, necessitates the urgent development of sustainable alternatives to traditional Portland cement.

Calcium carbonate ($CaCO_3$) emerges as a promising candidate for low-carbon construction materials due to its unique dual role: it serves as both a primary component in cement replacement strategies and a key player in carbon sequestration through mineral carbonation (Plummer & Busenberg, n.d.). Unlike conventional cement production, which releases CO_2, mineral carbonation actively captures atmospheric CO_2, offering a net-negative carbon pathway for construction materials (Power et al., 2013). $CaCO_3$ exists in multiple forms: three crystalline (CC) polymorphs (calcite, aragonite, vaterite) and amorphous phases (ACC), each with distinct properties affecting material performance and carbonation efficiency. The polymorph distribution directly influences mechanical strength, durability, and CO_2 uptake capacity, making precise control over polymorph formation critical for optimizing sustainable construction materials.

Despite extensive research on individual $CaCO_3$ phases, significant gaps remain in understanding how elemental substitutions commonly present in cement systems (Mg, Fe, Al, Si, Na, K) affect the thermodynamic stability and transformation pathways between polymorphs and amorphous phases. Current knowledge is primarily based on pure $CaCO_3$ systems under idealized conditions, limiting the applicability to real-world cement environments. Furthermore, while experimental studies provide valuable insights, they are often limited by the difficulty of controlling and characterizing transient amorphous phases and rapid transformation processes. The complex interplay between thermodynamic driving forces and kinetic barriers in multi-component systems requires a comprehensive computational approach that can bridge atomic-scale phenomena with macroscopic material properties. Existing computational studies have typically focused on single methods (e.g., DFT for crystalline phases) or limited compositional ranges, lacking the systematic integration needed to develop predictive models for engineering applications. This fragmented approach prevents the rational design of $CaCO_3$-based materials with tailored properties for specific construction applications.

This project aims to bridge these knowledge gaps by developing a comprehensive computational framework that integrates quantum mechanical, classical molecular dynamics, and thermodynamic modelling approaches to:

- Elucidate substitution effects on $CaCO_3$ polymorph stability and ACC behaviour in multi-component systems relevant to construction materials.
- Characterize transformation pathways between amorphous and crystalline phases under varying environmental conditions.
- Establish a robust thermodynamic database for rational design of sustainable $CaCO_3$-based construction materials.

Funded by the European Union

“Funded by the European Union. Views and opinions expressed are, however, those of the author(s) only and do not necessarily reflect those of the European Union or the European Research Executive Agency (REA). Neither the European Union nor the granting authority can be held responsible for them.”

The outcomes will enable the optimization of mineral carbonation processes and guide the development of high-performance, carbon-negative construction materials, contributing to the decarbonization of the built environment while providing permanent CO_2 storage.

4. Objective/Aim

This deliverable was prepared to share preliminary thermodynamic results and data for the pure calcium carbonate polymorphs obtained using density functional theory (DFT) and to illustrate how magnesium incorporates into these phases and affects their relative stability. It provides an initial Gibbs-energy-based framework for equilibrium calculations using the GEMS software and for a deeper understanding of substitution mechanisms in $CaCO_3$.Therefore, it offers early insights into how these interactions influence the thermodynamic behaviour of both crystalline and amorphous forms within the $CaCO_3$–H_2O system. These results directly support the CONTRABASS objectives related to the thermodynamics and carbonation mechanisms of calcium-based binders, forming the basis for future $CaCO_3$–H_2O phase diagram construction and predictive modelling of CO_2 uptake as well as long-term material performance and stability.

The main objective of this deliverable is to generate a consistent Gibbs-energy dataset based on DFT calculations and a critical review of the available experimental data for $CaCO_3$ polymorphs (calcite, aragonite, vaterite) and their Mg-substituted variants, representing the most relevant guest-element interactions in cementitious environments. By evaluating structural, energetic, vibrational, and temperature-dependent properties, this deliverable provides the quantitative basis needed to

- understand insertion mechanisms of minor ions (starting with Mg) into $CaCO_3$ through their effects on free-energy landscapes,
- assess their impact on thermodynamic stability, mixing behavior, and polymorphic transitions across temperature and composition ranges,
- support $CaCO_3$–H_2O phase-diagram construction, dissolution equilibria, and carbonation modelling using GEMS, Factsage or any other Gibbs energy minimizer software in subsequent project stages and other work packages within the CONTRABASS network.

By defining how minor elements modify the Gibbs energies and consequently equilibrium relations of $CaCO_3$ phases in contact with water, this deliverable contributes to the broader CONTRABASS objective of designing CO_2-neutral and carbon-negative construction materials through controlled carbonation of calcium silicates and aluminates.

Funded by the European Union

"Funded by the European Union. Views and opinions expressed are, however, those of the author(s) only and do not necessarily reflect those of the European Union or the European Research Executive Agency (REA). Neither the European Union nor the granting authority can be held responsible for them."

5. Content of the deliverable

5.1 Literature Review

5.1.1. Calcium Carbonate Polymorphs

Calcium carbonate ($CaCO_3$) represents one of the most abundant minerals in the Earth's crust, occurring naturally in various polymorphic forms with distinct crystallographic structures. These polymorphs have attracted significant scientific and industrial interest due to their prevalence in geological formations, biological systems, and technological applications.

5.1.1.1. Structural Properties

- **Calcite**

Calcite is the most thermodynamically stable $CaCO_3$ polymorph under ambient conditions. It crystallizes in a trigonal–rhombohedral lattice belonging to the space group $R\overline{3}c$, where the crystal structure consists of alternating layers of Ca^{2+} cations and planar CO_3^{2-} groups stacked along the c-axis. Each Ca^{2+} is six-fold coordinated, forming a slightly distorted octahedron with Ca–O distances of ~2.35–2.36 Å (Brik, 2011). The CO_3^{2-} units are strictly planar, with C–O bond lengths around 1.28 Å and triangular symmetry (D_3h). The alternating Ca–CO_3 layering facilitates cleavage along the (104) plane, influencing mechanical behavior and dissolution kinetics. Calcite contains a single crystallographic distinct Ca site, which favors uniform substitution of similarly sized cations (e.g., Mg^{2+}), though limited by ionic size mismatch and lattice strain. Its symmetry, relatively open framework, and simple coordination environment contributes to calcite's ability to accommodate minor elemental substitutions—although small cations (Mg^{2+}) generate significant local distortions.

- **Aragonite**

Aragonite crystallizes in an orthorhombic lattice (space group Pnma) with a denser and more anisotropic atomic arrangement than calcite. Its structure is stabilized at higher pressures and in the presence of certain additives or impurities. The Ca^{2+} ions are nine-fold coordinated, forming an irregular polyhedron with Ca–O distances ranging from 2.42 to 2.65 Å. The CO_3^{2-} groups are planar but differently oriented relative to those in calcite, producing lower symmetry and more complex stacking (Caspi et al., 2005). Aragonite's higher density (≈2.94 g/cm³ vs. ≈2.71 g/cm³ for calcite) reflects its closer cation–anion packing, which reduces its capacity for certain substitutions. These structural features help explain aragonite's stabilization under high-pressure conditions and the observed effects of Mg^{2+} in shifting the calcite–aragonite stability boundary.

- **Vaterite**

Vaterite is the most structurally intriguing and least understood polymorph of calcium carbonates. Its history reflects more than a century of evolving crystallographic interpretations, driven by the difficulty of resolving its inherently disordered structure. Unlike calcite and aragonite, which were clearly resolved in the 20th century, vaterite has resisted definitive structural classification due to its metastability, nanoscale heterogeneity, and tendency to transform into more stable polymorphs.

Funded by the European Union

"Funded by the European Union. Views and opinions expressed are, however, those of the author(s) only and do not necessarily reflect those of the European Union or the European Research Executive Agency (REA). Neither the European Union nor the granting authority can be held responsible for them."

The earliest crystallographic investigations of vaterite revealed diffraction patterns that did not fit any simple unit cell. Researchers observed broad, diffuse reflections suggesting a pseudo-hexagonal lattice. Work by Kamhi (1963) and earlier mineralogists showed that vaterite exhibited lattice parameters resembling a hexagonal pseudo cell (G. Sun et al., 2025), but attempts to refine it using classical crystallography consistently failed due to peak broadening and missing reflections. These early studies concluded that:

- vaterite is not describable by a single long-range-ordered unit cell,
- the observed diffraction corresponds to averaged symmetry, not true atomic positions,
- significant disorder must exist in the Ca and CO_3 sublattices.

This pseudo-hexagonal cell became the starting point for decades of structural proposals. Following the pseudo cell interpretation, researchers attempted to refine vaterite into higher-symmetry space groups (Demichelis et al., 2012; G. Sun et al., 2025).

Key contributions include :

- Pnma orthorhombic models and Ama2 variants, derived from fits to microcrystalline powders.
- C2/c monoclinic models, capturing subtle distortions in the carbonate layers.
- Well-defined hexagonal $P6_522$ structure derived from computational techniques.
- Attempts to explain peak splitting and diffuse scattering through stacking disorder.

However, these models struggled to reproduce all observed peaks, especially weak reflections and superlattice features. As experimental techniques improved, vaterite increasingly appeared to possess multiple local motifs rather than a uniform periodic arrangement. In 2013, Kabalah-Amitai et al. published a landmark study showing that vaterite crystals actually contain two interspersed structural domains, explaining why single-phase models always fell short (Kabalah-Amitai et al., 2013). However, such incorporation often destabilizes vaterite further**,** accelerating transformation to calcite. Moreover, local variations in Ca coordination (6–8 oxygen atoms) offer multiple insertion environments**,** unlike calcite or aragonite. Thus, vaterite's unique structural history directly informs its behavior in cementitious and carbonation systems.

5.1.1.2. Amorphous Calcium Carbonates

Amorphous calcium carbonate (ACC) is a non-crystalline phase of $CaCO_3$ with no long-range atomic order, typically considered a metastable precursor to crystalline polymorphs. ACC can exhibit diverse hydration states, which strongly influence its stability, solubility, and transformation kinetics to crystalline phases (Radha et al., 2012). Due to its transient nature, thermodynamic characterization of ACC remains challenging; however, it generally exhibits higher Gibbs free energy compared to crystalline forms, promoting rapid transformation into crystalline polymorphs under ambient conditions.

5.1.1.3. Thermodynamic Stability

The relative thermodynamic stability of $CaCO_3$ polymorphs follows a well-established hierarchy under ambient conditions, with calcite and aragonite exhibiting relatively equivalent stabilities, and vaterite representing the least stable polymorph (Jamieson, 1953). This stability sequence is quantitatively reflected in their standard molar free energies of formation (ΔH_f) at 25°C and 1 atm; calcite (~ -1207 kJ/mol), aragonite (~ -1207 kJ/mol), and vaterite (-1203.99 kJ/mol) (Jamieson,

Funded by the European Union

"Funded by the European Union. Views and opinions expressed are, however, those of the author(s) only and do not necessarily reflect those of the European Union or the European Research Executive Agency (REA). Neither the European Union nor the granting authority can be held responsible for them."

1953). Similarly, Christ, Hostetler, and Siebert derived standard Gibbs free energies of formation of -270,144 ± 375 cal.mol^{-1} (-1,130.28 ± 1.57 kJ/mol) for calcite and -269,926 ± 375 cal.mol^{-1} (-1,129.37 ± 1.57 kJ/mol) for aragonite, again indicating extremely small differences (Morton & McKelvey, n.d.). The small differences in Gibbs free energy between polymorphs with ΔG (aragonite-calcite) of -1.14±0.013 kJ/mol and ΔG (vaterite-calcite) of -2.9±0.2 (Wolf et al., 1996, 2000), demonstrate the fine thermodynamic balance that allows metastable phases to form and persist under certain conditions.

5.2 Methodology

5.2.1 Density Functional Theory

The first step of the methodological workflow consists of Density Functional Theory (DFT) calculations designed to obtain fully relaxed structures, electronic energies, and ground-state properties for both pure and substituted $CaCO_3$ phases. All calculations are performed using the Vienna Ab Initio Simulation Package (VASP) (Kresse & Furthmüller, 1996), employing the SCAN meta-GGA exchange functional, which is well-established for its high accuracy in predicting structural parameters, ground-state energies, and polymorph energetics of carbonate minerals (J. Sun et al., 2015). Structural optimizations are conducted for the three primary $CaCO_3$ polymorphs—calcite, aragonite, and vaterite—and their Mg-substituted analogues. Convergence is ensured through systematic testing of k-point meshes (Monkhorst & Pack, 1976) plane-wave energy cutoffs, ionic relaxation settings, and stress/force convergence thresholds. These steps guarantee accurate determination of equilibrium volumes, lattice constants, bond environments, and formation energies. Substituted structures are generated to assess the influence of guest elements (Mg as the primary case), capturing the local distortions and energetics relevant to cementitious systems.

5.2.2 Phonon Calculations

To evaluate the temperature-dependent thermodynamics of $CaCO_3$ polymorphs and their substituted structures, lattice vibrational calculations are performed with the Phonopy code using using the finite-displacement method on SCAN-optimized geometries, with additional refinements using the PBEsol functional for comparison to ensure accurate vibrational responses (Togo & Tanaka, 2015). The phonon calculations include non-analytical corrections (NAC), enabled through the computation of the high-frequency dielectric tensor and Born effective charges which are essential for correctly reproducing LO–TO splitting in polar materials such as carbonates.
Within the harmonic approximation (HA), phonons are computed by assuming that atoms oscillate around their equilibrium positions in a quadratic potential, yielding phonon frequencies, phonon densities of states, and vibrational thermodynamic quantities such as $C_v(T)$, $S(T)$, and the vibrational free energy $F_{vib}(T)$ at fixed volume. While the harmonic model provides reliable predictions at low temperatures and for rigid lattices, it does not account for thermal expansion or anharmonic effects. To capture these effects, the quasi-harmonic approximation (QHA) is employed, in which phonon calculations are repeated at a set of expanded and compressed volumes, an equation of state (e.g., Vinet or Birch–Murnaghan) is fitted, and Gibbs free energies $G(T, P)$ are obtained as a function of temperature. The combined harmonic–quasi-harmonic framework enables the determination of thermal expansion, $C_p(T)$, entropy and enthalpy trends, and polymorphic transition temperatures, thereby producing Gibbs-energy datasets for the solid

Funded by the European Union

"Funded by the European Union. Views and opinions expressed are, however, those of the author(s) only and do not necessarily reflect those of the European Union or the European Research Executive Agency (REA). Neither the European Union nor the granting authority can be held responsible for them."

phases suitable for constructing $CaCO_3$–H_2O phase diagrams and assessing the thermodynamic influence of minor-element substitutions.
All computational settings are summarized in Table 1.

Table 1 DFT parameters used for the calculation of ground states, and Phonon calculations parameters used for the calculation of high-temperature properties.

	PARAMETER	*VALUE / DESCRIPTION*
DFT FRAMEWORK	Code	VASP 6.3.2
	Exchange–Correlation Functional	SCAN (meta-GGA), PBEsol for refinement
	Pseudopotentials	PAW (VASP standard) *O_GW_new* *Ca_sv* *Mg_sv* *C*
	Precision	Accurate (PREC = Accurate)
	Energy Cutoff	700 eV
	K-point Mesh	Γ-centered *Calcite* 6x6x2 *Aragonite* 3x2x1 *Vaterite Pnma* 3x2x2 *Vaterite* $P2_1c$ 2x3x2 *Vaterite* $P6_522$ 2x2x1
	Threshold energy change between successive self-consistent field (SCF) cycles	$\Delta E \leq 1\times10^{-8}$ eV
	Algorithm	Conjugate Gradient
	Ionic relaxation loop condition	$F \leq 1\times10^{-5}$ eV/Å
PHONOPY FRAMEWORK	Supercells	*Calcite* 2×2×2 (240 atoms) *Aragonite* 2×2×2 (160 atoms) *Vaterite* Dependent on structural model *Substituted Structures* equivalent to their pure structures
	Threshold energy change between successive self-consistent field (SCF) cycles	$\Delta E \leq 1\times10^{-8}$ eV
	Charge Density Accuracy	Precision Mode
	Vibrational Quantities	Phonon DOS, $C_v(T)$, $S(T)$, $F_{vib}(T)$
	QHA Volume Range	±5% around equilibrium (7–9 volumes)
	Equation of State (EOS)	Vinet (preferred), Birch–Murnaghan (checked)
	Output Quantities	$G(T)$, $C_p(T)$, thermal expansion, $S(T)$, $H(T)$
	Temperature Range	0–1200 K

Funded by the European Union

"Funded by the European Union. Views and opinions expressed are, however, those of the author(s) only and do not necessarily reflect those of the European Union or the European Research Executive Agency (REA). Neither the European Union nor the granting authority can be held responsible for them."

5.3 Methodology Validation

As an essential first step, the accuracy of the SCAN (Strongly Constrained and Appropriately Normed) functional was evaluated for predicting the structural properties of the three $CaCO_3$ polymorphs—calcite, aragonite, and vaterite. The goal of this validation was to ensure that SCAN provides sufficiently precise lattice parameters and interatomic distances to serve as the foundation for subsequent phonon, thermodynamic, and substitution-energy calculations.

The computed lattice constants and unit-cell volumes obtained with SCAN were benchmarked against experimental crystallographic data and compared to values previously reported using other density functionals (LDA, PBE, PBEsol, B3LYP). As summarized in Table 2, SCAN consistently produced lattice parameters with the smallest deviations from experiment across the three polymorphs. We note that all DFT-relaxed structural parameters in Table 2 correspond to 0K calculations, whereas the experimental lattice constants were measured at room temperature; however, the close agreement between the two indicates that thermal expansion effects are small and that SCAN maintains a high degree of predictive accuracy.

Table 2 Unit cell parameters a, b and c (Å), unit cell volume V (Å^3), and mean C–O and Ca-O distances (Å) of the pure polymorphs of CaCO3, obtained from previous experimental data, Literature DFT calculations using different functionals, and from our DFT calculations using SCAN functional.

	Experimental	Calculations			SCAN
		LDA	PBE	B3LYP	
Calcite (Valenzano et al., n.d.)					
a, c (Å)	4.989, 17.059	4.960, 16.424	5.039, 17.402	5.037, 17.330	5.006, 16.990
V (Å3)	369.414	350	382.7	368.85	368.85
dC-O (Å)	1.282	1.2834	1.2978	1.2878	1.28
dCa-0 (Å)	2.359	2.3143	2.3907	2.3907	2.36
		LDA	GGA	B3LYP2	
Aragonite (Medeiros et al., 2006)					
a, b, c (Å)	4.962, 5.743, 7.969	4.893, 5.523, 7.850	5.015, 5.790, 8.032	5.017, 5.790, 7.901	4.95, 5.68, 7.945
V (Å3)	227.08	212.14	233.22	229.535	223.32
dC-O (Å)	1.282			1.2857	1.28
dCa-0 (Å)	2.528			2.5604	2.47
			PBEsol		
Vaterite Pnma (Ulian et al., 2021)					
a, b, c (Å)	4.13, 7.15, 8.48		4.431, 6.609, 8.503		4.432, 6.593, 8.514
V (Å3)	227.08		246.76		248.79
dC-O (Å)	--		1.292		1.285
dCa-0 (Å)	--		2.358		2.365
			PBEsol		
Vaterite P6522 (Ulian et al., 2021)					
a, c (Å)	7.1443, 25.35		7.1206, 25.439		7.28, 25.56
V (Å3)	1121.5		1117.1		1174.59
dC-O (Å)	--		1.293		1.3
dCa-0 (Å)	--		2.359		2.395

For calcite, SCAN reproduced the a and c lattice constants with deviations of only 0.35% and 0.40%, respectively—substantially more accurate than those obtained with alternative functionals, which show deviations ranging from 0.58% to 3.72% (Medeiros et al., 2006). Similar agreement was observed for aragonite, where SCAN reduced the typical over- or under-estimations found in LDA and GGA functionals. For vaterite, where crystallographic uncertainties are inherently larger, the SCAN-derived cell parameters remained within the narrow range of values reported for the

Funded by the European Union

"Funded by the European Union. Views and opinions expressed are, however, those of the author(s) only and do not necessarily reflect those of the European Union or the European Research Executive Agency (REA). Neither the European Union nor the granting authority can be held responsible for them."

proposed Pnma and $P6_522$ structural models. SCAN also accurately reproduced key interatomic distances, particularly the Ca–O coordination environment and C–O bond lengths in the carbonate groups. Deviations were extremely small—below 0.02% for C–O and 0.05% for Ca–O distances in both calcite and aragonite. In comparison, literature results based on LDA display Ca–O errors up to 1.89%, while PBE and B3LYP show errors exceeding 1% for the same metric (Brik, 2011; Ulian & Valdrè, 2022). This reinforces the capability of SCAN to capture both ionic and covalent bonding characteristics in $CaCO_3$ with high fidelity.

5.4 Zero Kelvin Energetics

The static ground-state energies $E0$ of the $CaCO_3$ polymorphs and relevant Mg-containing carbonate phases were obtained from fully relaxed DFT calculations using the SCAN functional. For comparison purposes, the ground state for calcite and aragonite was computed using the PBEsol GGA functional as well. These energies correspond to the 0K electronic internal energy per formula unit, without thermal or vibrational contributions. To obtain the correct thermodynamic reference at 0K for the pure polymorphs, zero-point vibrational energies (ZPE) were computed using lattice dynamics phonon calculations within the harmonic approximation. The resulting 0K Gibbs energy for each pure phase is calculated as:

$$G^0=E^0+ZPE$$

where the zero-point energy is given by

$$ZPE=\frac{1}{2}\sum_I \hbar\omega_I$$

evaluated over all phonon modes in the primitive cell. Because the entropy vanishes at 0K and the PV term for solids under ambient pressure is negligible, this expression is equivalent to the standard enthalpy at 0K. As seen in Table 3, based on the ZPE-corrected Gibbs energies calculated with SCAN, calcite and aragonite have close relative stabilities with a difference of 0.04 ($eV/f.u$) in their ground state energy. Similarly, the energy difference calculated with PBEsol is 0.02 ($eV/f.u$). All vaterite structural models lie 3–5 kJ/mol higher in energy than calcite, consistent with their known metastability. All the vaterite candidates show similar stability.

Table 3 Zero-Kelvin Ground-State Energies, ZPE-Corrected Gibbs Free Energies, and Zero-Kelvin Standard Formation Enthalpies of $CaCO_3$ Polymorphs obtained using SCAN and PBEsol functionals.

	Structure	E^0 $(eV/f.u)$	$G^0(eV/f.u)$	$H^0_f\,(KJ/mol)$
SCAN	Calcite	-50.836	-50.316	-1182.04
	Aragonite	-50.852	-50.352	-1185.51
	Vaterite Pnma	-50.772	-50.282	-1178.76
	Vaterite $P6_522$	-50.763	-50.273	-1177.89
	Vaterite $P2_1c$	-50.789	-50.289	-1179.43
PBEsol	Calcite	-39.1	-38.6	-1101.1
	Aragonite	-39.075	-38.58	-1099.6

The substitution 0K energetics summarized in Table 4 reveal distinct trends in the stability of $Ca_{1-x}Mg_xCO_3$ solid solutions across the major $CaCO_3$ polymorphs. For the substituted phases, ZPE is not yet available, hence, in Table 4, non-corrected Energies were used as the best approximation, which is acceptable knowing that ZPE differences between related Carbonate phases are typically modest compared to their formation energies.

Funded by the European Union

"Funded by the European Union. Views and opinions expressed are, however, those of the author(s) only and do not necessarily reflect those of the European Union or the European Research Executive Agency (REA). Neither the European Union nor the granting authority can be held responsible for them."

Table 4 Ground state energy E^0 $(eV/f.u)$ and formation energy from elements $\boldsymbol{H_f^O(KJ/mol)}$ of the different $Ca_{1-x}Mg_x(CO_3)$ structures, Magnesite structure, and Dolomite and it's substituted end members, and the heats of mixing $\Delta E^0{}_{mix}(KJ/mol)$ for the intermediate substitutions per structure obtained using SCAN.

Structure	Formula	$E^0(eV/f.u)$	$H_f^O(KJ/mol)$	$\Delta E^0 mix\ (KJ/mol)$
	$CaCO_3$	-50.84	-1232.2	-
	$Ca_{5/6}Mg_{1/6}CO_3$	-49.71	-1198.6	17.19
	$Ca_{4/6}Mg_{2/6}CO_3$	-48.59	-1165.0	34.19
Calcite	$Ca_{0.5}Mg_{0.5}CO_3$	-48.04	-1186.6	-3.9
	$Ca_{2/6}Mg_{4/6}CO_3$	-46.35	-1098.4	67.89
	$Ca_{1/6}Mg_{5/6}CO_3$	-45.23	-1064.9	84.99
	$MgCO_3$	-45.17	-1133.4	-
Magnesite	$MgCO_3$	-45.14	-1130.80	--
	$CaCO_3$	-50.49	-1198.8	
Dolomite	$CaMg(CO_3)_2$	-48.05	-2374.9	-37.15
	$MgCO_3$	-44.84	-1101.9	
	$CaCO_3$	-50.85	-1233.8	
	$Ca_{0.75}Mg_{0.25}CO_3$	-49.01	-1168.3	21.16
Aragonite	$Ca_{0.5}Mg_{0.5}CO_3$	-47.49	-1133.7	11.5
	$Ca_{0.25}Mg_{0.75}CO_3$	-45.49	-1052.5	48.3
	$MgCO_3$	-44.37	-1056.5	
	$CaCO_3$	-50.77	-1226.0	
	$Ca_{0.75}Mg_{0.25}CO_3$	-49.26	-1192.2	-17.4
Vaterite Pnma	$Ca_{0.5}Mg_{0.5}CO_3$	-47.31	-1116.7	6.8
	$Ca_{0.25}Mg_{0.75}CO_3$	-46.16	-1117.2	-45.0
	$MgCO_3$	-44	-1020.9	
Vaterite $P6_522$	$CaCO_3$	-50.76	-1225.2	
	$Ca_{5/6}Mg_{1/6}CO_3$	-49.7	-1197.3	-8.48
	$Ca_{4/6}Mg_{2/6}CO_3$	-48.7	-1175.5	-23.0
	$Ca_{0.5}Mg_{0.5}CO_3$	-41.54	-559.4	556.8
	$Ca_{2/6}Mg_{4/6}CO_3$	-46.4	-1103	23.1
	$Ca_{1/6}Mg_{5/6}CO_3$	-45.3	1071.5	-27.93
	$MgCO_3$	43.86	-1007.3	
Vaterite $P2_1C$	aCO_3	-50.79	-1227.7	
	$Ca_{0.75}Mg_{0.25}CO_3$	-49.3	-1196.1	-19.3
	$Ca_{0.5}Mg_{0.5}CO_3$	-47.62	-1146.2	-20.31
	$Ca_{0.25}Mg_{0.75}CO_3$	-46	-1101.7	-26.8
	$MgCO_3$	-44.03	-1024.1	

Funded by the European Union

"Funded by the European Union. Views and opinions expressed are, however, those of the author(s) only and do not necessarily reflect those of the European Union or the European Research Executive Agency (REA). Neither the European Union nor the granting authority can be held responsible for them."

Formation enthalpies were derived from the 0K energies using:

$$H_f/f.u = E^{tot} - (1-x)E^{Ca} - xE^{Mg} - E^{C} - \frac{3}{2}E^{O_2}$$

In calcite, Mg incorporation is generally thermodynamically unfavourable, as indicated by positive mixing energies across most compositions and a maximum destabilization near x≈0.83, consistent with the well-known limited solubility of Mg in the calcite lattice. A slight stabilization is observed at x=0.5 ($\Delta E^0{}_{mix}$=−3.9 kJ/mol), suggesting that intermediate substitution levels may benefit from local ordering effects of Mg on the Ca sublattice. As shown in Fig. 1, the mixing-energy profile in Calcite exhibits a shallow minimum at x=0.5, with mixing energies rising sharply toward both Mg-rich and Ca-rich limits. This characteristic shape indicates that only intermediate Mg contents offer slight energetic preference, while most other compositions are destabilized. A comparable trend was reported by Elstnerová et al.**,** whose DFT calculations likewise showed that only the x=0.5 configuration yields a small energetic stabilization, whereas all other Mg contents increase the energy of calcite (Elstnerová et al., 2010).

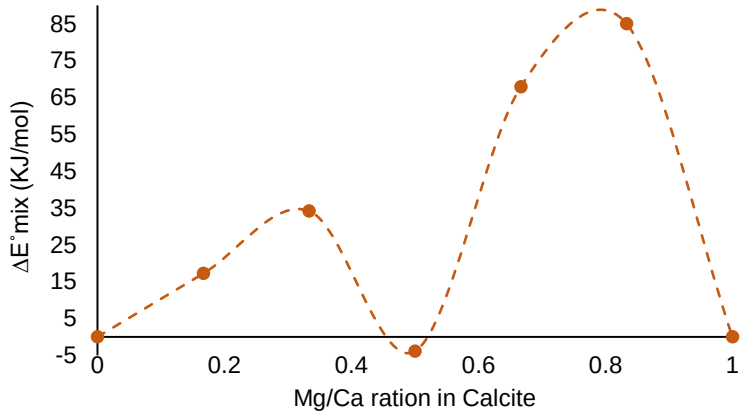

Fig.1 Mixing energies $\Delta E^0{}_{mix}$ (KJ/mol) as function of Mg/Ca substitution ratio in Calcite.

It is important to distinguish between randomly substituted calcite ($Ca_{0.5}Mg_{0.5}CO_3$) of space group $R\bar{3}c$ and the ordered dolomite structure ($CaMg(CO_3)_2$) with the related space group $R\bar{3}$. It is also important to note that in the table, the reported value for dolomite corresponds to two formula units ($CaMg(CO_3)_2$), whereas the half-substituted calcite model contains only one $CaCO_3$ formula unit with 50% Mg substitution. Consequently, the dolomite end-members can be viewed as one formula unit of fully ordered Ca–Mg carbonate, making its energetics directly comparable once normalized per $CaCO_3$ unit. This ordered structure in dolomite shows a more negative formation energy (-1187.4 KJ/mol) than randomly substituted calcite (-1186.6 KJ/mol), indicating that the ordered arrangement of Ca and Mg cations provides additional thermodynamic stabilization. This explains why dolomite forms as a distinct mineral phase in nature rather than just existing as Mg-substituted calcite (Hossain et al., 2011), despite their similar compositions. Aragonite, with its larger nine-fold Ca coordination, shows uniformly positive mixing energies (11–48 kJ/mol), indicating that Mg substitution is strongly unfavourable and supporting the experimental observation that aragonite accommodates little to no Mg at low temperature (Alruopn, n.d.). The vaterite polymorphs display structure-dependent behaviour: the Pnma and $P2_1c$ models show generally negative or weakly positive mixing energies, suggesting moderate Mg solubility and highlighting the structural flexibility of these metastable phases, whereas the $P6_522$ model exhibits both moderate stabilization at low substitution levels and a large positive outlier at x = 0.5, likely reflecting structural distortions or an insufficiently relaxed configuration at this composition. Overall, these non–ZPE-corrected results

Funded by the European Union

"Funded by the European Union. Views and opinions expressed are, however, those of the author(s) only and do not necessarily reflect those of the European Union or the European Research Executive Agency (REA). Neither the European Union nor the granting authority can be held responsible for them."

demonstrate that Ca–Mg mixing is non-ideal, dominated by strong ionic-size and coordination effects, with favourable ordering only in the dolomite structure and limited solubility in calcite and certain vaterite variants. This thermodynamic behaviour provides a quantitative foundation for predicting Ca–Mg partitioning, phase stability boundaries, and carbonation pathways in $CaCO_3$–$MgCO_3$ systems relevant to hydrated cement environments.

5.5 Thermodynamics of pure $CaCO_3$

The thermodynamic parameters shown in Table 6 obtained from our DFT calculations show excellent overall agreement with modelled values derived from experimental data for the stable $CaCO_3$ polymorphs (Lothenbach et al., 2019; Myers et al., 2015), while providing internally consistent values for the metastable vaterite structures. Across all SCAN-based harmonic and quasi-harmonic calculations, vaterite polymorphs consistently emerge as the least stable $CaCO_3$ phase, in full agreement with experimental thermodynamics. The more subtle question concerns the energetic separation between calcite and aragonite. Experimentally, there has been reports of virtually identical standard molar enthalpies of formation for both polymorphs ($\Delta H_f\,^0_{298}$ ≈ -1207±0.05 kJ/mol) and Gibbs energies differing by only ~1 kJ/mol (-1129±0.02 vs. -1128±0.02 kJ/mol) (Königsberger et al., 1999; Nan et al., 2007; Wolf et al., 1996). This near-degeneracy is reflected in our DFT results: SCAN yields $\Delta H_f\,^0_{298}$ = -1212.6 kJ/mol for calcite and -1215.1 kJ/mol for aragonite, with corresponding Gibbs energies of -1115.3 and -1120.5 kJ/mol. Although slightly more negative than experiment, the SCAN deviations remain small 4–8 kJ/mol in $\Delta H_f\,^0_{298}$ and 8–12 kJ/mol in $\Delta G_f\,^0_{298}$, corresponding to errors on the order of 0.5–1%. Such accuracy is exceptionally good for first-principles thermodynamics and strongly indicates that SCAN captures both the absolute and relative stabilities of calcite and aragonite. In contrast, absolute PBEsol formation enthalpies and Gibbs energies deviate more strongly from experiment, as expected for a GGA functional; however, PBEsol remarkably captures the relative stability between calcite and aragonite with high fidelity, yielding $\Delta G_f\,^0_{298}$ differences of only ~1–2 kJ/mol—essentially identical to experimental transitional energetics, confirming the internal consistency of GGA-level descriptions of $CaCO_3$ polymorphs (Gavryushkin et al., 2021).

The experimental standard molar entropies of calcite and aragonite show considerable variability across the literature, reflecting differences in calorimetric techniques, low-temperature extrapolations, and correction schemes. For calcite, published values range from 90 to 93 $J{\cdot}mol^{-1}{\cdot}K^{-1}$, corresponding to an experimental uncertainty of roughly ±3 $J{\cdot}mol^{-1}{\cdot}K^{-1}$ (4%). Aragonite shows a similarly wide spread, with reported entropies between 87 and 91 $J{\cdot}mol^{-1}{\cdot}K^{-1}$, giving an uncertainty of ±4 $J{\cdot}mol^{-1}{\cdot}K^{-1}$ (3–4%). The bar charts in Figure 2, visually demonstrate this. Within this context, the SCAN- and PBEsol-derived entropies fall comfortably inside the experimental uncertainty envelope. SCAN yields 85.4 $J \cdot mol^{-1} \cdot K^{-1}$ for calcite and 93.1 $J \cdot mol^{-1} \cdot K^{-1}$ for aragonite—both lying near the center of the experimentally observed ranges. PBEsol gives slightly higher values for aragonite but still remains well within the experimental scatter, while it gives a more accurate value for calcite. This agreement indicates that the small systematic differences introduced by the choice of exchange–correlation functional are minor compared to the intrinsic spread in experimental measurements.

Funded by the European Union

"Funded by the European Union. Views and opinions expressed are, however, those of the author(s) only and do not necessarily reflect those of the European Union or the European Research Executive Agency (REA). Neither the European Union nor the granting authority can be held responsible for them."

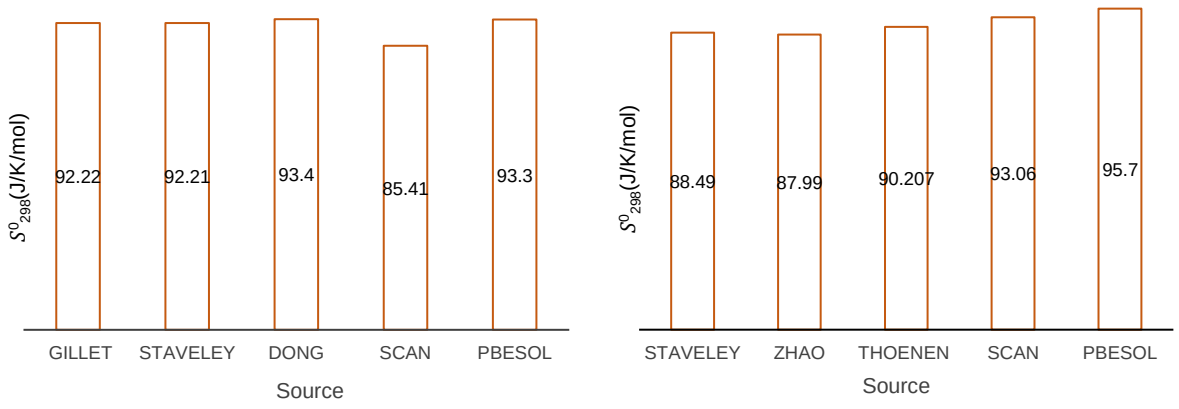

Fig. 2 Entropy S^0_{298} $(J/K/mol)$ of calcite and aragonite respectively, obtained from previous experimental data of different sources, and from our phonon calculations using SCAN and PBEsol functionals.

For the heat-capacity functions, all $C_p(T)$ curves were fitted to the polynomial form

$$Cp(T)=a_0+a_1T+a_2T^{-2}+a_3T^{-0.5}$$

QHA-derived $C_p(T)$ values were used where available, while HA-based $C_v(T)$ functions served as a proxy when QHA data were not accessible. The fitted polynomial coefficients reproduce the phonon-derived heat-capacity trends over 50–1200 K with low residuals (typically <1–2 $J/mol \cdot K$), ensuring full compatibility with the GEMS thermodynamic framework and enabling analytical integration to obtain consistent S(T), H(T), and G(T) functions.

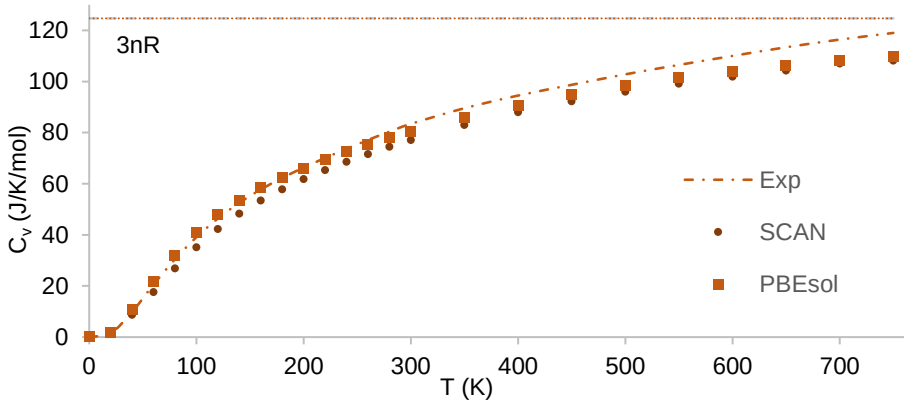

Fig. 3 Heat capacity at constant volume $C_v(T)$ (J/mol/K) of calcite obtained from our calculations using SCAN and PBEsol and previous experimental data (CattP et al., n.d.) as function of temperature (K).

Moreover, Figure 3 demonstrates the variation of the calculated heat capacity $C_v(T)$ $(J/mol/K)$ using SCAN and PBEsol in comparison to experimentally obtained ones as function of Temperature (K) for calcite. Notably, our results for calcite are in excellent agreement with those reported in the work of Gillet, which also employed harmonic phonon calculations; the deviation between our computed $C_v(T)$ values and theirs is less than 0.25% across the full temperature range for both functionals (Gillet et al., 1996). In that same study, it was shown that the harmonic approximation tends to systematically underestimate experimental $C_v(T)$ values, particularly at higher temperatures, due

Funded by the European Union

"Funded by the European Union. Views and opinions expressed are, however, those of the author(s) only and do not necessarily reflect those of the European Union or the European Research Executive Agency (REA). Neither the European Union nor the granting authority can be held responsible for them."

to its neglect of anharmonic effects. This was also reflected in the study by Price (Price, G. D., 1993), where the heat capacity of aragonite was calculated using quasi-harmonic approaches. Similarly, our values are underestimated compared to CattP's due to neglect of anharmonic effects (CattP et al., n.d.). Overall, the computed $C_v(T)$ values show excellent agreement with experiment, confirming the validity of the phonon methodology; notably, the PBEsol results overlap with the experimental curve up to about 350 K, further demonstrating that the vibrational spectrum is being captured accurately even with a simpler functional.

Overall, the computational dataset in Table 6 provides a robust and internally consistent set of thermodynamic parameters suitable for direct implementation in GEMS. Calcite and aragonite match experimental values extremely well, while the vaterite polymorphs show trends consistent with their metastability. Minor corrections may be applied to Cp for the HA-only structures, but the core $\Delta H_f\,^{0}_{298}$, $\Delta G_f\,^{0}_{298}$, and V° values are solid and reliable for thermodynamic modeling.

6. Conclusion

This deliverable contributes to the broader context of understanding the thermodynamics of calcium carbonate phases and their role in CO_2 uptake, carbonation mechanisms, and long-term stability of calcium-based binders. The problem addressed here is the absence of consistent, Gibbs-energy-based thermodynamic data for $CaCO_3$ polymorphs derived from first-principles calculations, as well as the need to quantify how magnesium incorporation affects the stability hierarchy among crystalline and amorphous $CaCO_3$ phases. The objective of the task was therefore to generate a complete and internally consistent thermodynamic dataset for calcite, aragonite, and vaterite polymorphs using DFT and lattice-dynamics methods, to evaluate their relative energetics, and to prepare these results in a format suitable for implementation into GEMS.

The methodology combined density functional theory (SCAN and PBE exchange-correlation functionals), harmonic and quasi-harmonic phonon calculations, thermodynamic integration, and the fitting of heat-capacity curves to a GEMS suitable format allowing analytical evaluation of (H(T)), (G(T)), and (S(T)). QHA data were used wherever available to capture thermal expansion effects, while HA results provided complementary enthalpy, entropy, and vibrational contributions. All volumes were converted to molar volumes, and the oxygen chemical potential was standardised to ensure consistent formation energies across phases.

The key findings show that SCAN-based QHA and HA calculations reproduce experimental thermodynamics of calcite and aragonite with high accuracy: $\Delta H_f\,^{0}_{298}$ and $\Delta G_f\,^{0}_{298}$ values fall within 1% of experimental references, molar volumes match measured values within uncertainties, and $C_p(T)$ fits reproduce the phonon-derived data with small residuals. For vaterite polymorphs, the energetics fall within the expected window for metastable $CaCO_3$, and their predicted $C_p(T)$, S, and V values are realistic despite the inherent limitations of harmonic calculations. The results confirm the expected stability ordering and provide the first DFT-consistent Gibbs-energy dataset for evaluating Mg substitution effects across these phases.

The evaluation of the results shows that the methodology is robust and that the produced thermodynamic parameters are sufficiently accurate to be used for phase-diagram construction, carbonation modelling, and further integration into GEMS. Limitations arise mainly from the harmonic treatment of vibrational effects in some vaterite structures, which leads to underestimations of Cp and S, and from the absence of full QHA sampling for $P6_522$ vaterite.

Funded by the European Union

"Funded by the European Union. Views and opinions expressed are, however, those of the author(s) only and do not necessarily reflect those of the European Union or the European Research Executive Agency (REA). Neither the European Union nor the granting authority can be held responsible for them."

Nevertheless, these shortcomings do not affect the overall energetic trends or the applicability of the dataset.

The optimal solution identified here is the combination of SCAN-based QHA for Cp(T) and HA for enthalpy and entropy corrections, as it yields the best balance between computational cost and thermodynamic accuracy. Overall, the planned objectives of the task have been fully achieved: a coherent, DFT-based thermodynamic database for $CaCO_3$ polymorphs has been established, prepared in GEMS-compatible form, and validated against literature.

This work has broader implications for other CONTRABASS tasks focused on carbonation mechanisms, CO_2 uptake, and predictive modelling of binder evolution. The dataset produced here can be directly used in $CaCO_3$–H_2O phase diagram calculations, stability assessments of substituted phases, and future modelling of Mg-bearing carbonates. Future work should extend the quasi-harmonic analysis to all vaterite structures, incorporate explicit Mg substitutions in supercell models, evaluate amorphous $CaCO_3$ phases, and integrate aqueous species to complete the $CaCO_3$–$MgCO_3$–H_2O thermodynamic framework required for whole-system carbonation simulations.

Funded by the European Union

"Funded by the European Union. Views and opinions expressed are, however, those of the author(s) only and do not necessarily reflect those of the European Union or the European Research Executive Agency (REA). Neither the European Union nor the granting authority can be held responsible for them."

Table 6. Standard thermodynamic properties at 25 °C and 1 atm for calcium carbonate phases. The dataset format is consistent with the GEMS version of the PSI/Nagra 12/07 TDB (Lothenbach et al., 2019).

Phase	Method	$\Delta G_f{}^0{}_{298}$ (kJ/mol)	$\Delta H_f{}^0{}_{298}$ (kJ/mol)	S^0_{298} $(J/mol/K)$	a_0 $(J/mol/K)$	a_1 $(J/mol/K^2)$	a_2 $(J \cdot K/mol)$	a_3 $(J/mol/K\text{^}0.5)$	V^0_{298} (cm^3/mol)	$C_P(T)$ $(J/mol \cdot K)$	$C_v(T)$ $(J/mol \cdot K)$
Calcite	SCAN QHA (Cp(T), S, V), SCAN HA (ΔH, ΔG, Cv)	-1115.3	-1212.6	85.75	134.5	0.022	104851	-1133.9	37.2	76.83	77.44
Aragonite	SCAN QHA (Cp(T)), SCAN HA (ΔH, ΔG, Cv, S)	-1120.5	-1215.1	93.06	153.5	0.0012	106768.4	-1277	33.8	81.3	77.84
Vaterite p21/c	SCAN QHA (ΔG, Cp, V, S)	-1111.6	--	82.2	377.7	-0.15	697007.7	-4219.6	38.1	83.03	--
Vaterite Pnma	SCAN QHA (Cp(T), S), SCAN HA (ΔH, ΔG, Cv)	-1110.18	-1211.4	81.2	139.4	0.0073	117720.6	-1207.75	37.1	73.08	66.15
Vaterite $P6_522$	SCAN HA (ΔH, ΔG, Cv, S)	-1110.3	-1209.4	78.38	--	--	--	--	--	--	71.6
Calcite	PBEsol HA (ΔH, ΔG, Cv, S)	-1102.2	-1134.9	93.3	--	--	--	--	--	--	80.4
Aragonite	PBEsol HA (ΔH, ΔG, Cv, S)	-1100.1	-1132	95.7	--	--	--	--	--	--	80.3

Funded by the European Union

"Funded by the European Union. Views and opinions expressed are, however, those of the author(s) only and do not necessarily reflect those of the European Union or the European Research Executive Agency (REA). Neither the European Union nor the granting authority can be held responsible for them."

7. References

Alruopn, P. L. (n.d.). Structural refinementsof dolomite and a magnesiancalcite andimplicationsfor dolomiteformation in the marineenvironment.

Brik, M. G. (2011). First-principles calculations of structural, electronic, optical and elastic properties of magnesite MgCO3 and calcite CaCO3. Physica B: Condensed Matter, 406(4), 1004–1012. https://doi.org/10.1016/j.physb.2010.12.049

Caspi, E. N., Pokroy, B., Lee, P. L., Quintana, J. P., & Zolotoyabko, E. (2005). On the structure of aragonite. Acta Crystallographica Section B Structural Science, 61(2), 129–132. https://doi.org/10.1107/S0108768105005240

CattP, M., Pavese, A., & Price, G. D. (n.d.). Thermodynamic Properties of C a C O 3 Calcite and Aragonite: A Quasi-Harmonic Calculation.

Demichelis, R., Raiteri, P., Gale, J. D., & Dovesi, R. (2012). A new structural model for disorder in vaterite from first-principles calculations. CrystEngComm, 14(1), 44–47. https://doi.org/10.1039/C1CE05976A

Elstnerová, P., Friák, M., Fabritius, H. O., Lymperakis, L., Hickel, T., Petrov, M., Nikolov, S., Raabe, D., Ziegler, A., Hild, S., & Neugebauer, J. (2010). Ab initio study of thermodynamic, structural, and elastic properties of Mg-substituted crystalline calcite. Acta Biomaterialia, 6(12), 4506–4512. https://doi.org/10.1016/j.actbio.2010.07.015

Gavryushkin, P. N., Belonoshko, A. B., Sagatov, N., Sagatova, D., Zhitova, E., Krzhizhanovskaya, M. G., Rečnik, A., Alexandrov, E. V., Medrish, I. V., Popov, Z. I., & Litasov, K. D. (2021). Metastable structures of $CaCO_3$ and their role in transformation of calcite to aragonite and postaragonite. Crystal Growth & Design, 21(1), 65–74. https://doi.org/10.1021/acs.cgd.0c00589

Gillet, P., McMillan, P., Schott, J., Badro, J., & Grzechnik, A. (1996). Thermodynamic properties and isotopic fractionation of calcite from vibrational spectroscopy of 18O-substituted calcite. Geochimica et Cosmochimica Acta, 60(18), 3471–3485. https://doi.org/10.1016/0016-7037(96)00178-0

Hossain, F. M., Dlugogorski, B. Z., Kennedy, E. M., Belova, I. V., & Murch, G. E. (2011). First-principles study of the electronic, optical and bonding properties in dolomite. Computational Materials Science, 50(3), 1037–1042. https://doi.org/10.1016/j.commatsci.2010.10.044

Jamieson, J. C. (1953). Phase Equilibrium in the System Calcite-Aragonite. The Journal of Chemical Physics, 21(8), 1385–1390. https://doi.org/10.1063/1.1699228

Kabalah-Amitai, L., Mayzel, B., Kauffmann, Y., Fitch, A. N., Bloch, L., Gilbert, P. U. P. A., & Pokroy, B. (2013). Vaterite Crystals Contain Two Interspersed Crystal Structures. Science, 340(6131), 454–457. https://doi.org/10.1126/science.1232139

Königsberger, E., Königsberger, L.-C., & Gamsjäger, H. (1999). Low-temperature thermodynamic model for the system Na2CO3−MgCO3−CaCO3−H2O. Geochimica et Cosmochimica Acta, 63(19–20), 3105–3119. https://doi.org/10.1016/S0016-7037(99)00238-0

Kresse, G., & Furthmüller, J. (1996). Efficient iterative schemes for ab initio total-energy calculations using a plane-wave basis set. Physical Review B, 54(16), 11169–11186. https://doi.org/10.1103/PhysRevB.54.11169

Lothenbach, B., Kulik, D. A., Matschei, T., Balonis, M., Baquerizo, L., Dilnesa, B., Miron, G. D., & Myers, R. J. (2019). Cemdata18: A chemical thermodynamic database for hydrated Portland cements and alkali-activated materials. Cement and Concrete Research, 115, 472–506. https://doi.org/10.1016/j.cemconres.2018.04.018

Medeiros, S. K., Albuquerque, E. L., Maia, F. F., Caetano, E. W. S., & Freire, V. N. (2006). Structural, electronic, and optical properties of CaCO3 aragonite. Chemical Physics Letters, 430(4–6), 293–296. https://doi.org/10.1016/j.cplett.2006.08.133

Miller, S. A., Horvath, A., & Monteiro, P. J. M. (2016). Readily implementable techniques can cut annual CO_2 emissions from the production of concrete by over 20%. Environmental Research Letters, 11(7), 074029. https://doi.org/10.1088/1748-9326/11/7/074029

Monkhorst, H. J., & Pack, J. D. (1976). Special points for Brillouin-zone integrations. Physical Review B, 13(12), 5188–5192. https://doi.org/10.1103/PhysRevB.13.5188

Morton, R. C. B., & McKelvey, V. E. (n.d.). UNITED STATES DEPARTMENT OF THE INTERIOR.

Myers, R. J., Lothenbach, B., Bernal, S. A., & Provis, J. L. (2015). Thermodynamic modelling of alkali-activated slag cements. Applied Geochemistry, 61, 233–247. https://doi.org/10.1016/j.apgeochem.2015.06.006

Nan, Z., Shi, Z., Qin, M., Hou, W., & Tan, Z. (2007). Formation Process and Thermodynamic Poperties of Calcite. Chinese Journal of Chemistry, 25(5), 592–595. https://doi.org/10.1002/cjoc.200790111

Plummer, L. N., & Busenberg, E. (n.d.). The solubilities of calcite, aragonite and vaterite in COrHzO solutions between 0 and 9O"C, and an evaluation of the aqueous model for the system CaC03-CO*-Hz0.

Power, I. M., Harrison, A. L., Dipple, G. M., Wilson, S., Kelemen, P. B., Hitch, M., & Southam, G. (2013). Carbon Mineralization: From Natural Analogues to Engineered Systems. Reviews in Mineralogy and Geochemistry, 77(1), 305–360. https://doi.org/10.2138/rmg.2013.77.9

Price, G. D. (1993). Thermodynamic properties of CaCO3 calcite and aragonite: A quasi-harmonic calculation.

Radha, A. V., Fernandez-Martinez, A., Hu, Y., Jun, Y.-S., Waychunas, G. A., & Navrotsky, A. (2012). Energetic and structural studies of amorphous Ca1−Mg CO3·nH2O (0 ⩽x⩽ 1). Geochimica et Cosmochimica Acta, 90, 83–95. https://doi.org/10.1016/j.gca.2012.04.056

Sun, G., Liu, X., Lian, B., & Wang, S. (2025). Research Progress on Vaterite Mineral and Its Synthetic Analogs. Minerals,

Funded by the European Union

"Funded by the European Union. Views and opinions expressed are, however, those of the author(s) only and do not necessarily reflect those of the European Union or the European Research Executive Agency (REA). Neither the European Union nor the granting authority can be held responsible for them."

15(8), 796. https://doi.org/10.3390/min15080796
Sun, J., Ruzsinszky, A., & Perdew, J. P. (2015). Strongly Constrained and Appropriately Normed Semilocal Density Functional. Physical Review Letters, 115(3), 036402. https://doi.org/10.1103/PhysRevLett.115.036402
Togo, A., & Tanaka, I. (2015). First principles phonon calculations in materials science. Scripta Materialia, 108, 1–5. https://doi.org/10.1016/j.scriptamat.2015.07.021
Ulian, G., Moro, D., & Valdrè, G. (2021). Benchmarking dispersion-corrected DFT methods for the evaluation of materials with anisotropic properties: Structural, electronic, dielectric, optical and vibrational analysis of calcite (CaCO3, space group R̄c). Phys. Chem. Chem. Phys., 23(34), 18899–18907. https://doi.org/10.1039/D1CP02673A
Ulian, G., & Valdrè, G. (2022). Structural and elastic behaviour of aragonite at high-pressure: A contribution from first-principle simulations. Computational Materials Science, 212, 111600. https://doi.org/10.1016/j.commatsci.2022.111600
Valenzano, L., Torres, F. J., Doll, K., Pascale, F., Zicovich-Wilson, C. M., & Dovesi, R. (n.d.). Ab Initio Study of the Vibrational Spectrum and Related Properties of Crystalline Compounds; the Case of CaCO3 Calcite.
Wolf, G., Königsberger, E., Schmidt, H. G., Königsberger, L.-C., & Gamsjäger, H. (2000). Thermodynamic Aspects of the Vaterite-Calcite Phase Transition. Journal of Thermal Analysis and Calorimetry, 60(2), 463–472. https://doi.org/10.1023/A:1010114131577
Wolf, G., Lerchner, J., Schmidt, H., Gamsjäger, H., Königsberger, E., & Schmidt, P. (1996). Thermodynamics of CaCO3 phase transitions. Journal of Thermal Analysis, 46(2), 353–359. https://doi.org/10.1007/BF02135013

Funded by the European Union

"Funded by the European Union. Views and opinions expressed are, however, those of the author(s) only and do not necessarily reflect those of the European Union or the European Research Executive Agency (REA). Neither the European Union nor the granting authority can be held responsible for them."